

# S<sup>3</sup>LAM: Structured Scene SLAM

Mathieu Gonzalez<sup>1</sup>, Eric Marchand<sup>2</sup>, Amine Kacete<sup>1</sup> and Jerome Royan<sup>1</sup>

**Abstract**—We propose a new general SLAM system that uses the semantic segmentation of objects and structures in the scene. Semantic information is relevant as it contains high level information which may make SLAM more accurate and robust. Our contribution is threefold: i) A new SLAM system based on ORB-SLAM2 that creates a semantic map made of clusters of points corresponding to objects instances and structures in the scene. ii) A modification of the classical Bundle Adjustment formulation to constrain each cluster using geometrical priors, which improves both camera localization and reconstruction and enables a better understanding of the scene. iii) A new Bundle Adjustment formulation at the level of clusters to improve the convergence of classical Bundle Adjustment. We evaluate our approach on several sequences from a public dataset and show that, with respect to ORB-SLAM2 it improves camera pose estimation.

## I. INTRODUCTION

The goal of SLAM is to construct a map of the environment seen by a moving camera while simultaneously estimating the pose of the camera. It is a fundamental algorithm for robotics and augmented reality (AR) that has seen many improvements during the past few years and is now able to correctly estimate the pose of a camera in small and large scale scenes [1], [2], [3]. The map can take different forms, sparse [1], semi-dense [2], dense [3] but is always purely geometric and lacks semantic meaning which is an important information to make SLAM more robust and accurate [4]. Furthermore the lack of semantic information may limit the applications that can make use of this map. For example mobile robots may need to recognize objects in the scene for path planing. AR applications can as well use semantic information to overlay contextual information on specific parts of the image and virtually interact with some objects [5]. With the rise of CNNs, methods for object detection [6] and segmentation [7], [8] are now available for practical use applications. Several studies have been conducted to merge those methods with SLAM by fusing multiple segmentations to obtain consistent semantic maps [9], [10]. Furthermore a semantic comprehension of the environment may improve SLAM itself at several stages of the pipeline, more particularly for long term re-localization [11], [12], [13], [14], [15] and dynamic objects handling [16], [5], [17], [18]. Some works use objects as high level landmarks [19], [20], [21], [22], [23]. To do so, they can make use of specific objects [20], [23], [24], [25] at the disadvantage

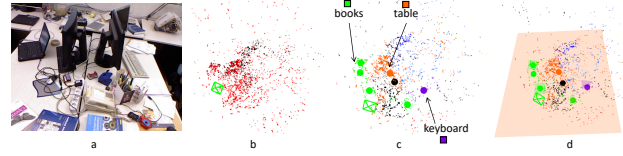


Fig. 1. (a) frame from the sequence fr1\_desk. Comparison of (b) a map built by ORB-SLAM2, (c) a map of clusters where each cluster centroid is represented with a big ball (books are in green, table in orange, keyboard in purple, other objects are not used) and (d) a map of clusters with estimated planes.

of requiring a specialised object pose estimation algorithm [26], [27], [28]. To discard this constraint some works propose to represent objects in a generic way using for example quadrics [21], [22] or 3D bounding boxes [19] and use a generic object detector. Planes can be seen as specific objects that are numerous in many environments and can be also integrated into SLAM [21], [29], [30], [31], [32], [33].

In this paper we present a monocular SLAM system, called S<sup>3</sup>LAM for Structured Scene SLAM, based on the state-of-the-art ORB-SLAM2 [1] that can segment generic objects in the scene using a panoptic segmentation CNN, namely detectron2 [34]. We propose to create a new scene representation in which objects are seen as clusters of triangulated 3D points with semantic information. This allows us to create a semantic map with object instances and structures as shown in figure 1. Using this map of clusters we make use of simple prior information about object classes to constrain the map, which improves camera localization, and provides a higher level semantic map as shown in figure 1. Furthermore we propose a new Bundle Adjustment (BA) formulation at the clusters level. This new BA associated with classical BA improves its convergence and reduces computation time.

In summary contributions presented in this paper are:

- A general SLAM system that can detect object instances in the scene to create clusters of 3D points corresponding to such objects.
- A monocular SLAM system that can infer structures from clusters and constrain the map given such estimations.
- A new BA formulation at the level of objects to both improve camera localization accuracy and to decrease the complexity of BA.
- An evaluation of our approach on sequences from a public dataset which demonstrates the benefits of our method, both in term of camera pose precision and computational efficiency.

The rest of the paper is described as follows. First we

<sup>1</sup> Mathieu Gonzalez, Amine Kacete and Jerome Royan are with the Institute of Research and Technology b-com {mathieu.gonzalez, amine.kacete, jerome.royan}@b-com.com

<sup>2</sup> Eric Marchand is with Univ Rennes, Inria, IRISA, CNRS, Rennes, France, Eric.Marchand@irisa.fr

describe related work on classical and semantic SLAM. Then we describe our approach to create a structured map and make use of those structures. Finally we demonstrate the benefits of our approach on several sequences from a public dataset.

## II. RELATED WORK: SEMANTIC SLAM

The problem of visual SLAM has been studied for decades and multiple systems are now able to precisely estimate the pose of a camera within a reconstructed map [1], [2], [3]. Classically the approach consists in estimating the pose of the camera and the map of the environment by maximizing the likelihood of those variables given image measurements. ORB-SLAM2 [1] is considered to be the current State-Of-The-Art of visual SLAM. In their system the measurements are sparse ORB [35] keypoints extracted from images. The system is divided in threads which estimate the pose of the camera and the 3D position of map points. This strategy inspired from [36], [37] allows to refine the estimations with a local Bundle Adjustment [38] which minimizes the reprojection error of map points. LSD-SLAM [2] directly uses pixels on high gradient regions of the image to estimate the pose of the camera and build a semi-dense map. The pose of the keyframes are as well refined using pose graph optimization. Semantic information can be calculated using CNNs and then injected into a SLAM map [10], [39], [40], [9], [41]. For example SemanticFusion [10] is a dense SLAM which computes a pixelwise probability distribution for each frame and fuse the results for each surfel using a bayesian approach, which gives a semantic dense map. The semantic map can then be used to improve the SLAM. Semantic information can be useful for long term relocalization as segmentation CNNs are more invariant and global than traditional keypoints features [11], [12], [13], [14], [15]. The work of [12] is the first to use only semantic information for relocalization by minimizing the distance between a reprojected map point with a given semantic class and the nearest same class area in the image. Similarly [13] proposes to compute a semantic consistency score corresponding to the number of points projected in the correct semantic area. This score is then used to downweight outliers in a RANSAC scheme. Semantic information may allow a SLAM system to know which objects are static or eventually dynamic [16], [18], [17], [42], [43], [41] which improves SLAM robustness in real scenarios. Indeed most systems make the assumption that the scene is mostly static, detecting dynamic objects as outliers with RANSAC, but those approaches fail in highly dynamic environments. [16] proposes to segment images and to mask out a set of classes considered to be a priori dynamic. They use also depth information can to detect additional dynamic objects and refine the segmentation. This approach improves camera pose estimation in highly dynamic environments, however when a priori dynamic objects are static it can deteriorate the performances. [41] uses semantic information to mask out people and computes a moving consistency score on each segment to deduce whether or not it is moving. Semantic information is as well used to build a dense semantic map.

Object based SLAM systems consist in detecting objects in the scene and inserting them in the map to add constraints between frames, thus adding temporal consistency [20], [24], [23], [19], [21], [22]. This can bring robustness to the SLAM and accuracy by having access to the objects scale. Those systems can be divided into two main categories. The first one consist of object based SLAM systems that use specific objects [20], [23], [24], [25]. SLAM++ [20] is one of the most well known object based SLAM. The approach estimates the 6 DoF pose of objects in the scene from RGB-D images. Each estimated object is rendered using its mesh and the pose of the camera is estimated by minimizing the ICP error with the live depth frame. SLAM++ builds a graph of keyframes and objects as a map and optimizes the pose graph. On the other hand some works propose to model objects using quadrics [21], [22] or 3D bounding boxes [19]. QuadricSLAM [22] uses quadrics for localization and mapping. The main idea is to generate quadrics from 2D bounding boxes predicted by an object detection network. The quadrics parameters and keyframe poses are then refined in a BA so that the 2D projection of quadrics tightly fits the 2D bounding boxes.

Planar SLAM systems consist in detecting planar structures in the scene and using them as high level landmarks [29], [30], [21], [44], [33], [31], [45], [32]. The goal is threefold: first, planes are usually large structures and can thus constrain different parts of a scene without visual overlap. Second, some man-made planar structures do not contain valuable information for keypoint based SLAM, for example white walls, hence using planes as landmarks can enable tracking and mapping in those challenging cases. Finally detecting planes in the scene allows to get a better understanding of its physical structure which can enable interaction, contrary to a simple sparse point cloud. [29] proposes to use only planes as landmarks. Planes are extracted from RGB-D images and injected in a graph based SLAM using a minimal representation which allows them to be optimized with keyframes trajectory. [45] follows the same strategy and proposes a real-time plane-based SLAM on CPU. [21] uses planes to constrain the SLAM map. Planes are estimated from 3 different neural networks that estimate depth, normals and plane segmentation. From these redundant estimations planes are inserted in the map. The point-plane distance is then minimized within the BA. [30] proposes a monocular SLAM using planes to constrain the structure of the scene. Planes are estimated using a RANSAC on the whole map, thus they need to be large enough. In-plane points are then projected onto the estimated planes and both 2D plane points as well as plane parameters are optimized to minimize the reprojection error.

## III. S<sup>3</sup>LAM: A CLUSTER BASED SLAM

In S<sup>3</sup>LAM the map is represented as a set of point clouds, grouped according to the object instance they belong. Our goal is to use prior knowledge about these objects to enrich the SLAM, improve camera pose estimation as well as to obtain a better representation of the structure of the scene. Our

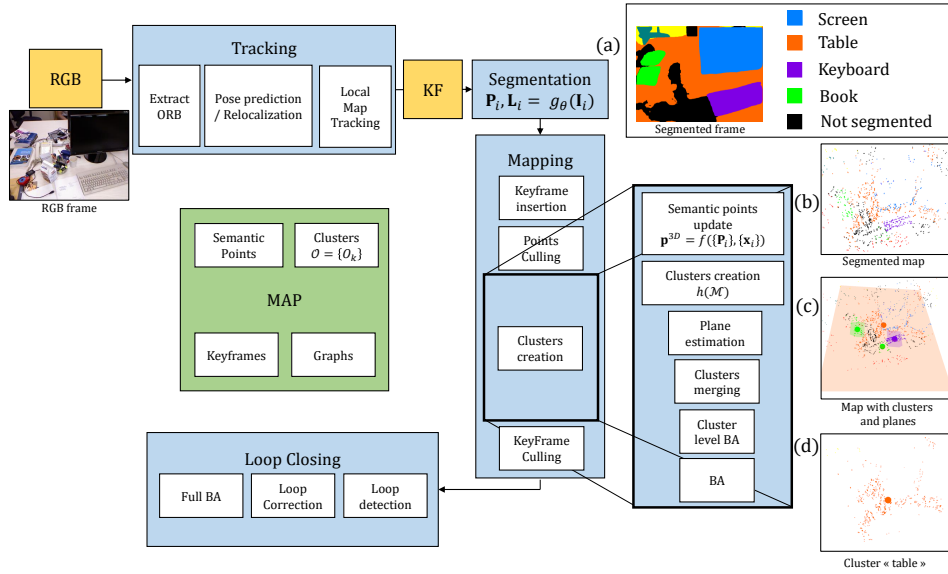


Fig. 2. Illustration of our pipeline integrated in [1]. (a) A CNN segments the keyframes, (b) the output of the CNN allows us to compute the probability distribution of map points, (c) we create clusters of points based on their semantic class and fit planes for planar classes, (d) we apply our stratified BA on each cluster followed by a local BA.

goal is to estimate the pose of a monocular camera moving in 3D space, represented at time  $i$  by the 6 DoF transformation between world frame  $\mathcal{F}_w$  and camera frame  $\mathcal{F}_{c_i}$  with the homogeneous matrix that defines the transformation denoted  ${}^{c_i}\mathbf{T}_w \in SE(3)$ . The pipeline of our approach can be seen in figure 2. We segment each keyframe using a panoptic segmentation network. In the mapping thread we update the class distribution of map points using the output of the panoptic segmentation network. Segmented map points allow us to create semantic clusters. For some clusters of classes corresponding to planar objects a plane is fitted using the 3D points and a merging step avoids the creation of duplicated clusters. Our cluster level BA then refines camera poses and points position for each cluster, followed by local BA.

#### A. Clusters Creation.

In this section we show how we manage to cluster points, according to the object instance they belong using semantic information.

**Panoptic segmentation:** Unlike most recent works [21], [19] we do not consider object bounding boxes as input but rather the panoptic segmentation of the image. Panoptic segmentation is a combination of semantic segmentation where each pixel is classified in a given class and instance segmentation where multiple objects of the same class are segmented separately. While panoptic segmentation is harder and takes longer to obtain it allows us to naturally know which keypoints belong to detected objects. Indeed while bounding boxes give the coarse location and size of an object in the image they do not separate the object from the background within the box. Hence a refinement process is required [17]. Moreover contrary to object detection CNN, panoptic segmentation networks, like semantic segmentation networks, are not limited to objects and can segment whole

areas in the image, such as floor, which correspond to the global structure of the scene. However contrary to semantic segmentation networks, panoptic segmentation separates multiple instances of a single class, allowing to treat each object separately. The downside of the additional information brought by panoptic segmentation is its complexity, while object detectors can easily process to tens of images per second [6], most recent panoptic segmentation networks run only at 5 to 10 fps. However we do not need to segment images at frame rate. As shown in [10], segmenting frames with a low frequency leads to a small drop in mapping segmentation accuracy while allowing the SLAM to run in real time. Moreover panoptic segmentation is an active field of research and real time networks can be expected in the near future.

To represent the panoptic segmentation network we define a function  $g_\theta(\mathbf{I}_i) \rightarrow \mathbf{P}_i, \mathbf{L}_i$  which, given an RGB image at time  $i$ ,  $\mathbf{I}_i$  and  $\theta$ , the network parameters, yields a probability map  $\mathbf{P}_i \in [0, 1]^{W \times H \times C}$ . Thus for each pixel  $\mathbf{x}_j = (u_j, v_j)$  in the image we can obtain a probability distribution  $(\mathbf{P}_i(u_j, v_j, 1), \dots, \mathbf{P}_i(u_j, v_j, C))$  where  $\mathbf{P}_i(u_j, v_j, c)$  corresponds to the probability that this pixel belongs to class  $c$ . The second output of the network is the instance map  $\mathbf{L}_i \in \mathbb{N}^{W \times H}$  in which each object is segmented and given a unique id.

**Clusters creation:** Following the 2D segmentation, we define a function  $f(\{\mathbf{P}_i\}, \{\mathbf{x}_i\}) \rightarrow \mathbf{p}^{3D}$  where  $\{\mathbf{P}_i\}$  is a set of probability maps at different times,  $\{\mathbf{x}_i\}$  is a set of keypoints corresponding to one 3D point  ${}^w\mathbf{X}$  and  $\mathbf{p}^{3D} = (p_1, \dots, p_C)$  is its probability distribution. This function is the fusion of multiple observations and can be

<sup>1</sup> $W$  and  $H$  represent the width and height of an RGB image,  $C$  is the total number of semantic classes.

written using Bayes rule [10], equation (1).

$$p_c = \mathbb{P}(c|\{\mathbf{P}_i\}) = \frac{1}{Z} \mathbb{P}(c|\{\mathbf{P}_{i-1}\}) \mathbf{P}_i(u_i, v_i, c) \quad (1)$$

where  $c$  is the class label of  ${}^w\mathbf{X}$  and  $Z$  is a normalization factor. Hence  $f$  allows us to obtain a semantic map  $\mathcal{M} = \{({}^w\mathbf{X}, \mathbf{p}^{3D}, c^*, l)_j\}$ , where each point  ${}^w\mathbf{X}$  has a probability distribution  $\mathbf{p}^{3D}$ , an id  $l$  extracted from the instance map  $\mathbf{L}^i$  as well as a semantic class  $c^* = \underset{c}{\operatorname{argmax}} \mathbf{p}^{3D}$ .

Using this semantic map we can define a clustering function  $h(\mathcal{M}) \rightarrow \mathcal{O}$  where  $\mathcal{O}$  is a partition of  $\mathcal{M}$  in  $K$  clusters  $\mathcal{O} = \{O_{k,k \in [1,K]}\}$ . This function groups points according to their semantic class and instance. Each cluster can be defined as  $O_k = \{\{{}^w\mathbf{X}\}_{c_k}\}$  where  $\{{}^w\mathbf{X}\}$  is the position of a set of points belonging to the cluster and  $c_k$  is the cluster class.

### B. Cluster Bundle Adjustment.

In this section we propose a new BA strategy taking into account the clustering of points. Classical BA is done by solving equation 2 either on the whole set of map points and keyframes or on a subset defined by the covisibility of the current keyframe [1].

$${}^c\hat{\mathbf{T}}_w, {}^w\hat{\mathbf{X}} = \underset{{}^c\mathbf{T}_w, {}^w\mathbf{X}}{\operatorname{argmin}} \sum_{i,j} \rho(\|\mathbf{x}_{i,j} - \operatorname{proj}({}^c\mathbf{T}_w, {}^w\mathbf{X}_j)\|_{\Sigma_{i,j}}^2) \quad (2)$$

where  $\operatorname{proj}({}^c\mathbf{T}_w, {}^w\mathbf{X}_j)$  is the classical reprojection model of point  ${}^w\mathbf{X}_j$  in the  $i^{th}$  keyframe with pose  ${}^c\mathbf{T}_w$ ,  $\|\mathbf{x}\|_{\Sigma} = \sqrt{\mathbf{x}^T \Sigma^{-1} \mathbf{x}}$  denotes the Mahalanobis norm of  $\mathbf{x}$  with  $\Sigma$  the covariance matrix and  $\rho$  is a robust cost function [46]. Solving this equation is traditionally done using an iterative minimization algorithm like Gauss-Newton or Levenberg-Marquardt [38], [47]. Using the clusters of points defined in the previous section we propose to solve the BA on a subset of points corresponding to the  $k^{th}$  cluster:

$${}^c\hat{\mathbf{T}}_w, {}^w\hat{\mathbf{X}} = \underset{{}^c\mathbf{T}_w, {}^w\mathbf{X}}{\operatorname{argmin}} \sum_{i,j \in O_k} \rho(\|\mathbf{x}_{i,j} - \operatorname{proj}({}^c\mathbf{T}_w, {}^w\mathbf{X}_j)\|_{\Sigma_{i,j}}^2) \quad (3)$$

This formulation allows the algorithm to optimize points position and keyframes poses using many less points, which is much faster than solving the whole BA. However as less data is involved we can expect the local minima obtained to be higher than the one obtained using the classical BA. Thus we use the following strategy: we optimize (3) for every cluster in the map which allows to rapidly obtain a first sub optimal estimation. Then we refine this estimation using (2) but limiting the number of iterations to save computation time. We argue that this strategy improves the convergence rate of the BA. However some care must be taken for keyframes optimization. Indeed some clusters can contain only tens of points that are very localized in space. This can cause the keyframes pose to converge to bad local minima which makes the keyframes jitter in the map. To avoid this we require clusters to have a number of points higher than some threshold  $\tau$ . If this is not the case, all keyframes in (3) are fixed and only points are optimized.

### C. Map Optimization from structure estimation.

Most man-made objects can be approximated with a more or less complex geometrical model, from a simple plane or box to the exact 3D model of the object. The advantage of approximating objects is twofold. First, we can add constraints to the optimization process to improve pose estimation. Second, we obtain a more physically accurate representation of the world by understanding the structures within it, contrary to recent methods that use quadrics to represent objects, which only roughly represent the spatial extent of objects but not their shape [21], [22]. In our work as an example we propose to model some objects using planes. Not only do we model large surfaces such as tables, walls or floor but we also model small objects like keyboards and books. Planes are represented using the classical 4D vector  $\pi = (a, b, c, d)^T$  with  $\|\pi\|_2 = 1$  [29] and planar points  $\mathbf{X}$  in homogeneous coordinates satisfy the following equation:  $\pi^T \mathbf{X} = 0$ . Contrary to most planar SLAM systems we do not need to use multiple specific CNNs [21] or depth [29] to estimate plane parameters, which limit the applicability of those systems. Instead for each a priori planar cluster, we fit a plane using the triangulated 3D points of this cluster in the world coordinates system. This is done using an SVD inside a RANSAC loop to make the estimation more robust to wrong classification and triangulation similarly to [30]. However contrary to [30] we are not limited to simple scenes with few very large planes. Indeed as we create semantic clusters we are able to fit planes even for small specific objects and thus we can apply our approach in a wider variety of scenes. Moreover the fitting procedure is made easier by the clustering and be done in near real-time compared to the 5 fps limitation in [30].

To avoid creating wrong planes that would corrupt the map, a plane is accepted if it is supported by enough inliers, which depends on the cluster class. For example, keyboards require at least 50 points to be inliers.

One way to add a structure constraint is to use a lagrangian multiplier [48], however this adds parameters that need to be estimated, thus we chose to include the constraint as a regularizer as can be seen in equation (4).

$${}^c\hat{\mathbf{T}}_w, {}^w\hat{\mathbf{X}} = \underset{{}^c\mathbf{T}_w, {}^w\mathbf{X}}{\operatorname{argmin}} \sum_{i,j} \rho(\|\mathbf{x}_{i,j} - \operatorname{proj}({}^c\mathbf{T}_w, {}^w\mathbf{X}_j)\|_{\Sigma_{i,j}}) + \sum_k \sum_{j \in O_k} \rho(\|\pi_k^w \mathbf{X}_j\|_{\sigma}) \quad (4)$$

where  $\|\pi_k^w \mathbf{X}_j\|$  is the 3D distance between the 3D point  ${}^w\mathbf{X}_j$  (in homogeneous coordinates) and the plane  $\pi_k$  which corresponds to the cluster  $O_k$ ,  $\sigma$  corresponds to its uncertainty, and  $\rho$  is a robust cost function (in our case the Huber loss).

Contrary to [30] we do not project 3D points in their plane as some clusters may not be perfectly planar. However the strength of the constraint can be tuned by changing the value of  $\sigma$ . Moreover contrary to [30] we do not optimize the planes, treating them as landmark but only use them as constraints on the map structure.

We optimize this equation using the framework g2o [49]. We build a classical BA graph. Then we add an unary constraint to each point belonging to a planar cluster. We consider those points to be outliers if their error is greater than the 95<sup>th</sup> percentile of a one-dimensional Chi-squared distribution. To account for points that would be outside of the local BA when a plane is fitted we chose to apply a global planar bundle adjustment after plane fitting. Furthermore to account for segmentation noise we remove from the cluster points that are too far from the plane.

#### IV. EXPERIMENTS

In this section we first present the implementation details of our approach, then we show on sequences from the TUM dataset [50] the validity of our method.

##### A. Implementation details

S<sup>3</sup>LAM runs at 20 fps and is based on the state of the art ORB-SLAM2 [1]. The optimization is done using the optimization framework g2o [49]. All the experiments are performed on a desktop computer with an Intel Xeon @3.7GHz with 16 Gb of RAM and an Nvidia RTX2070. The probability maps and instance maps for every frame in the datasets are pre-computed and stored. However this instance map is not temporally consistent, thus for each detected instance in  $\mathcal{L}^i$  we compute the IOU with all instances of the same class in  $\mathcal{L}^{i-1}$  and  $\mathcal{L}^{i-2}$  to track the id. We consider an instance to be well tracked if the IOU is above a threshold  $\tau_{i-1}=0.65$  for  $\mathcal{L}^{i-1}$  and  $\tau_{i-2}=0.4$  for  $\mathcal{L}^{i-2}$ . Using our simple tracking approach clusters are well defined, however when a cluster that has left the camera field of view for a few frames reappears in the image, the segmentation network creates a new instance, which leads to the creation of a new cluster. To avoid creating infinitely many clusters we define a merging function to fuse clusters together when the distance between their centroid is lower than a threshold  $\tau_{merge}$  and more than 80% of clusters points descriptors match. The value of the point-plane uncertainty  $\sigma$  is set constant to 100, which balances both errors as the value of the point-plane distance is around  $10^{-2}$  m while the reprojection error is around one pixel. The threshold for accepting a point as an inlier in the RANSAC is set to 5 mm except for the class *table* which is cluttered and not well segmented and thus is set at 2 mm.

**Datasets.** Our approach is evaluated on sequences from the TUM RGB-D dataset [50] which provides a set of RGB frames associated to their groundtruth pose.

**Metrics.** To account for the inherent stochasticity of ORB-SLAM2 we run each sequence 10 times and report the median of the RMSE of absolute trajectory error (ATE, defined in [50]) in the tables below. As our experiments are performed in a monocular setting, we scale and align the estimated trajectories with the ground truth as in [51].

##### B. Impact of the cluster level BA on pose error and computation time

In this section we study the impact of our new stratified BA formulation on pose error. We chose to limit the classical

BA to 2 iterations followed by 1 iteration without outliers to show that we can use less iterations than ORB-SLAM2 that uses 5 and 10 iterations. As we can see on the left of table I our cluster level BA associated with classical BA yields better results than ORB-SLAM2 on most sequences. On the right of the table we can see the average run time of the optimization procedure, computation time is decreased by 20 to 29%. To provide a better insight as to how our approach works we chose to study the BA cost function with and without cluster level BA. To do so we compute the average relative improvement of the cost function using our approach compared to classical BA at the first and last iteration. At the first iteration the average improvement is of 8% while at the last iteration it is of 0.5%. This shows that with our approach the first iteration starts at a way better minimum and reaches a slightly better one at the end, which explains why less iterations are required to reach it.

##### C. Impact of the planes constraints on pose error

In this section we study the impact of adding planar constraints to the classical BA formulation, using only planes robustly estimated from the 3D semantic map. We report the results of our experiments in table II. As we can see, planar constraints improve camera localization in most cases over ORB-SLAM 2 and [21] while we do not need to use multiple specific CNNs to fit planes. The most important improvement is obtained on almost perfectly planar scenes like *fr1\_floor* and *fr3\_nostr.text.near* which allow to easily fit planes. As we could expect using large planes gives better ATE improvements, the line *fr3\_nostr.text.near* (merged books) in table II shows our approach using a single plane for all book clusters, thus treating them as a single large cluster. An interesting way to improve our approach would thus to add plane-plane constraints to increase the spatial extent of small planes. The sequences *fr1\_xyz* and *fr1\_desk* show only a slight improvement as the main plane corresponding to a table is not well segmented and cluttered, yielding to a noisy estimation

To further show that the estimated map structure is coherent we compute the scalar product between pairs of normals that are supposed to be parallel at the end of a sequence (like pairs of books or books on a table for example). The minimum, maximum and median angles between normals are shown in table III. As we can see the estimated normals are pairwise coherent. Moreover the larger the planes are, the more points are extracted and the better the estimation is as visible in the last two lines of the table.

##### D. Qualitative analysis of S<sup>3</sup>LAM

We show in figure 3 some qualitative examples of maps obtained using our clustering approach compared to maps obtained using ORB-SLAM2 [1]. The goal of this figure is to show that the clusters and planes are well defined, to better see the effect of planes on the map quality we refer the reader to figure 4. To construct these maps we used the following classes: table, keyboard, book. As we can see every object present in the scene has been uniquely

Sequence	ATE (mm)		time (ms)	
	ORB-SLAM 2 [1]	S <sup>3</sup> LAM w. cluster level BA	ORB-SLAM2 [1]	S <sup>3</sup> LAM w. cluster level BA
fr1_xyz	9.2	9.2	36	28 [+20 %]
fr1_desk	13.9	13.8	38	27 [+29 %]
fr2_xyz	2.8	2.4	35	27 [+23 %]
fr3_nostr_text_near <sup>2</sup>	20.3	20.1	50	39 [+22%]

TABLE I

MEDIAN OF THE RMSE (MM) OF ATE FOR OUR MONOCULAR SLAM AGAINST ORB-SLAM2 [1] USING OUR CLUSTER LEVEL BA FORMULATION AND COMPUTATION TIMES WITH PERCENTAGE OF IMPROVEMENT OVER ORB-SLAM2 REPRESENTED IN BRACKETS. BEST RESULTS SHOWN IN GREEN, WORST RESULTS IN RED.

Sequence	ORB-SLAM2 [1]	Hosseinizadeh et al. [21] w. planes constraints	S <sup>3</sup> LAM w. planes constraints
fr1_xyz	9.2	10.3	8.8 [+4 %]
fr1_floor	18.1	16.9	14.7 [+13 %]
fr1_desk	13.9	12.9	13.2 [-2 %]
fr3_nostr_text_near <sup>2</sup>	20.3	Not available	15.3 [+25 %]
fr3_nostr_text_near <sup>2</sup> (merged books)	20.3	Not available	13.5 [+33 %]

TABLE II

MEDIAN OF THE RMSE (MM) OF ATE FOR OUR MONOCULAR SLAM AGAINST ORB-SLAM2 [1] AND HOSSEINZADEH ET AL. [21] USING PLANAR CONSTRAINTS. IMPROVEMENT OVER BEST SHOWN IN BRACKETS.

Sequence	max. angle	min. angle	med. angle
fr1_desk	3.6°	2.4°	2.9°
fr3_nostr_text_near	1.4°	0.8°	0.8°
fr3_nostr_text_near (merged books)	0.0°	0.0°	0.0°

TABLE III

MAXIMUM, MINIMUM AND AVERAGE VALUES OF ANGLES BETWEEN PLANE NORMALS. THE CLOSER TO 0 THE BETTER.

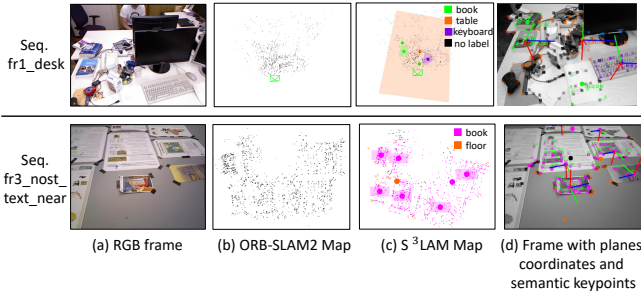


Fig. 3. Examples of maps created by our approach for 2 sequences from [50]. From left to right: (a) RGB input image from the sequence, (b) ORB-SLAM2 map, (c) S<sup>3</sup>LAM map, (d) Frame with planes normals projected in red, in plane vectors are shown in blue and green. Keypoints are as well shown with a color corresponding to their class.

clustered, leading to a more comprehensible and higher level map. We also show for each planar cluster the estimated planes, corresponding to the objects table, keyboard and book. Our approach yields a more physically accurate representation of the world, which can be easily used for augmented reality or robotics applications. In figure 4 we show a comparison of the map obtained with ORB-SLAM2 and the map obtained using our planar BA. As we can see on the right the lower part of the map corresponding to the floor (visible in orange in the bottom part of the map) is much more planar and coherent using our approach.

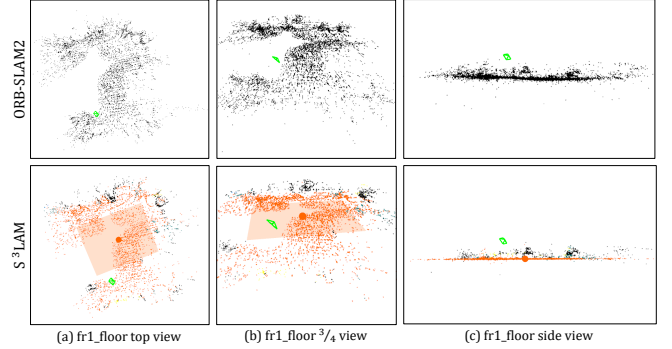


Fig. 4. Examples of map created by ORB-SLAM2 [1] (top) and our approach (bottom) for the sequence fr1\_floor. From left to right: (a) Map top view, (b) Map 3/4 view, (c) Map side view. As we can see on the side view the floor is more planar with our approach. Black points that are outside of the plane are points that have not been segmented as "floor" and thus do not undergo the planar constraint.

## V. CONCLUSION

In this paper we proposed a new monocular Semantic SLAM system called S<sup>3</sup>LAM. Our method uses the 2D panoptic segmentation of a sequence of RGB images to create clusters of 3D points according to their class and instance. This clustering allows us to propose a new cluster level Bundle Adjustment formulation which improves the convergence of classical BA, greatly reducing computation time. Furthermore, knowledge of semantic classes allows us to robustly estimate the structure of some clusters and modify the Bundle Adjustment formulation with structural constraints. We show on sequences from a public dataset that our approaches respectively lead to a reduced computation time and an improvement of camera pose estimation.

<sup>2</sup>For this sequence we disabled the loop closure to better study the impact of our approach.

## REFERENCES

- [1] R. Mur-Artal and J. D. Tardós, “ORB-SLAM2: An open-source SLAM system for monocular, stereo, and RGB-D cameras,” *IEEE Trans. on Robotics*, vol. 33, no. 5, pp. 1255–1262, 2017.
- [2] J. Engel, T. Schöps, and D. Cremers, “LSD-SLAM: Large-scale direct monocular SLAM,” in *European Conf. on computer vision*. Springer, 2014, pp. 834–849.
- [3] R. A. Newcombe, S. Izadi, O. Hilliges, D. Molyneaux, D. Kim, A. J. Davison, P. Kohi, J. Shotton, S. Hodges, and A. Fitzgibbon, “Kinectfusion: Real-time dense surface mapping and tracking,” in *2011 10th IEEE international symposium on mixed and augmented reality*, 2011, pp. 127–136.
- [4] C. Cadena, L. Carlone, H. Carrillo, Y. Latif, D. Scaramuzza, J. Neira, I. Reid, and J. J. Leonard, “Past, present, and future of simultaneous localization and mapping: Toward the robust-perception age,” *IEEE Trans. on robotics*, vol. 32, no. 6, pp. 1309–1332, 2016.
- [5] M. Runz, M. Buffier, and L. Agapito, “Maskfusion: Real-time recognition, tracking and reconstruction of multiple moving objects,” in *2018 IEEE International Symposium on Mixed and Augmented Reality (ISMAR)*, 2018, pp. 10–20.
- [6] J. Redmon, S. Divvala, R. Girshick, and A. Farhadi, “You only look once: Unified, real-time object detection,” in *IEEE Conf. on computer vision and pattern recognition*, 2016, pp. 779–788.
- [7] K. He, G. Gkioxari, P. Dollár, and R. Girshick, “Mask R-CNN,” in *IEEE Int. Conf. on computer vision*, 2017, pp. 2961–2969.
- [8] A. Kirillov, R. Girshick, K. He, and P. Dollár, “Panoptic feature pyramid networks,” in *IEEE/CVF Conf. on Computer Vision and Pattern Recognition*, 2019, pp. 6399–6408.
- [9] K. Tateno, F. Tombari, I. Laina, and N. Navab, “CNN-SLAM: Real-time dense monocular SLAM with learned depth prediction,” in *IEEE Conf. on Computer Vision and Pattern Recognition*, 2017, pp. 6243–6252.
- [10] J. McCormac, A. Handa, A. Davison, and S. Leutenegger, “Semanticfusion: Dense 3D semantic mapping with convolutional neural networks,” in *2017 IEEE Int. Conf. on Robotics and automation (ICRA)*, 2017, pp. 4628–4635.
- [11] J. L. Schönberger, M. Pollefeys, A. Geiger, and T. Sattler, “Semantic visual localization,” in *IEEE Conf. on Computer Vision and Pattern Recognition*, 2018, pp. 6896–6906.
- [12] C. Toft, C. Olsson, and F. Kahl, “Long-term 3D localization and pose from semantic labellings,” in *IEEE Int. Conf. on Computer Vision Workshops*, 2017, pp. 650–659.
- [13] C. Toft, E. Stenborg, L. Hammarstrand, L. Brynte, M. Pollefeys, T. Sattler, and F. Kahl, “Semantic match consistency for long-term visual localization,” in *European Conf. on Computer Vision (ECCV)*, 2018, pp. 383–399.
- [14] R. Arandjelović and A. Zisserman, “Visual vocabulary with a semantic twist,” in *Asian Conf. on Computer Vision*. Springer, 2014, pp. 178–195.
- [15] N. Kobyshev, H. Riemenschneider, and L. Van Gool, “Matching features correctly through semantic understanding,” in *2014 2nd Int. Conf. on 3D Vision*, vol. 1, 2014, pp. 472–479.
- [16] B. Bescos, J. M. Fàcil, J. Civera, and J. Neira, “DynaSLAM: Tracking, mapping, and inpainting in dynamic scenes,” *IEEE Robotics and Automation Letters*, vol. 3, no. 4, pp. 4076–4083, 2018.
- [17] J. Huang, S. Yang, T.-J. Mu, and S.-M. Hu, “ClusterVO: Clustering moving instances and estimating visual odometry for self and surroundings,” in *IEEE/CVF Conf. on Computer Vision and Pattern Recognition*, 2020, pp. 2168–2177.
- [18] B. Bescos, C. Campos, J. D. Tardós, and J. Neira, “DynaSLAM II: Tightly-coupled multi-object tracking and SLAM,” *IEEE Robotics and Automation Letters*, vol. 6, no. 3, pp. 5191–5198, 2021.
- [19] S. Yang and S. Scherer, “CubeSLAM: Monocular 3-d object SLAM,” *IEEE Trans. on Robotics*, vol. 35, no. 4, pp. 925–938, 2019.
- [20] R. F. Salas-Moreno, R. A. Newcombe, H. Strasdat, P. H. Kelly, and A. J. Davison, “SLAM++: Simultaneous localisation and mapping at the level of objects,” in *IEEE Conf. on computer vision and pattern recognition*, 2013, pp. 1352–1359.
- [21] M. Hosseinzadeh, K. Li, Y. Latif, and I. Reid, “Real-time monocular object-model aware sparse SLAM,” in *2019 Int. Conf. on Robotics and Automation (ICRA)*, 2019, pp. 7123–7129.
- [22] L. Nicholson, M. Milford, and N. Sünderhauf, “QuadricSLAM: Dual quadrics from object detections as landmarks in object-oriented SLAM,” *IEEE Robotics and Automation Letters*, vol. 4, no. 1, pp. 1–8, 2018.
- [23] D. Gálvez-López, M. Salas, J. D. Tardós, and J. Montiel, “Real-time monocular object SLAM,” *Robotics and Autonomous Systems*, vol. 75, pp. 435–449, 2016.
- [24] N. Fioraio and L. Di Stefano, “Joint detection, tracking and mapping by semantic bundle adjustment,” in *IEEE Conf. on Computer Vision and Pattern Recognition*, 2013, pp. 1538–1545.
- [25] J. Civera, D. Gálvez-López, L. Riazuelo, J. D. Tardós, and J. M. M. Montiel, “Towards semantic SLAM using a monocular camera,” in *2011 IEEE/RSJ Int. Conf. on Intelligent Robots and Systems*, 2011, pp. 1277–1284.
- [26] M. Rad and V. Lepetit, “BB8: A scalable, accurate, robust to partial occlusion method for predicting the 3D poses of challenging objects without using depth,” in *IEEE Int. Conf. on Computer Vision*, 2017, pp. 3828–3836.
- [27] M. Gonzalez, A. Kacete, A. Murienne, and E. Marchand, “L6dnet: Light 6 DoF network for robust and precise object pose estimation with small datasets,” *IEEE Robotics and Automation Letters*, 2021.
- [28] Y. Xiang, T. Schmidt, V. Narayanan, and D. Fox, “PoseCNN: A convolutional neural network for 6d object pose estimation in cluttered scenes,” *arXiv preprint arXiv:1711.00199*, 2017.
- [29] M. Kaess, “Simultaneous localization and mapping with infinite planes,” in *2015 IEEE Int. Conf. on Robotics and Automation (ICRA)*, 2015, pp. 4605–4611.
- [30] C. Arndt, R. Sabzevari, and J. Civera, “From points to planes - adding planar constraints to monocular SLAM factor graphs,” in *2020 IEEE/RSJ Int. Conf. on Intelligent Robots and Systems (IROS)*, 2020, pp. 4917–4922.
- [31] S. Yang, Y. Song, M. Kaess, and S. Scherer, “Pop-up SLAM: Semantic monocular plane SLAM for low-texture environments,” in *2016 IEEE/RSJ Int. Conf. on Intelligent Robots and Systems (IROS)*, 2016, pp. 1222–1229.
- [32] F. Servant, P. Houlrier, and E. Marchand, “Improving monocular plane-based SLAM with inertial measures,” in *2010 IEEE/RSJ Int. Conf. on Intelligent Robots and Systems*, 2010, pp. 3810–3815.
- [33] A. Concha and J. Civera, “Using superpixels in monocular SLAM,” in *2014 IEEE Int. Conf. on robotics and automation (ICRA)*, 2014, pp. 365–372.
- [34] Y. Wu, A. Kirillov, F. Massa, W.-Y. Lo, and R. Girshick, “Detectron2,” <https://github.com/facebookresearch/detectron2>, 2019.
- [35] E. Rublee, V. Rabaud, K. Konolige, and G. Bradski, “ORB: An efficient alternative to SIFT or SURF,” in *2011 Int. Conf. on computer vision*, 2011, pp. 2564–2571.
- [36] E. Mouragnon, M. Lhuillier, M. Dhome, F. Dekeyser, and P. Sayd, “Real time localization and 3D reconstruction,” in *2006 IEEE Computer Society Conf. on Computer Vision and Pattern Recognition (CVPR’06)*, vol. 1, 2006, pp. 363–370.
- [37] G. Klein and D. Murray, “Parallel tracking and mapping for small AR workshops,” in *2007 6th IEEE and ACM international symposium on mixed and augmented reality*, 2007, pp. 225–234.
- [38] B. Triggs, P. F. McLauchlan, R. I. Hartley, and A. W. Fitzgibbon, “Bundle adjustment—a modern synthesis,” in *International workshop on vision algorithms*. Springer, 1999, pp. 298–372.
- [39] X. Li and R. Belaroussi, “Semi-dense 3D semantic mapping from monocular SLAM,” *arXiv preprint arXiv:1611.04144*, 2016.
- [40] N. Sünderhauf, T. T. Pham, Y. Latif, M. Milford, and I. Reid, “Meaningful maps with object-oriented semantic mapping,” in *2017 IEEE/RSJ Int. Conf. on Intelligent Robots and Systems (IROS)*, 2017, pp. 5079–5085.
- [41] C. Yu, Z. Liu, X.-J. Liu, F. Xie, Y. Yang, Q. Wei, and Q. Fei, “DS-SLAM: A semantic visual SLAM towards dynamic environments,” in *2018 IEEE/RSJ Int. Conf. on Intelligent Robots and Systems (IROS)*, 2018, pp. 1168–1174.
- [42] H. Taira, I. Rocco, J. Sedlar, M. Okutomi, J. Sivic, T. Pajdla, T. Sattler, and A. Torii, “Is this the right place? geometric-semantic pose verification for indoor visual localization,” in *IEEE/CVF Int. Conf. on Computer Vision*, 2019, pp. 4373–4383.
- [43] M. Schorghuber, D. Steininger, Y. Cabon, M. Humenberger, and M. Gelautz, “SLAMANTIC-leveraging semantics to improve vslam in dynamic environments,” in *IEEE/CVF Int. Conf. on Computer Vision Workshops*, 2019.
- [44] S. Yang and S. Scherer, “Monocular object and plane SLAM in structured environments,” *IEEE Robotics and Automation Letters*, vol. 4, no. 4, pp. 3145–3152, 2019.
- [45] M. Hsiao, E. Westman, G. Zhang, and M. Kaess, “Keyframe-based

- dense planar SLAM,” in *2017 IEEE Int. Conf. on Robotics and Automation (ICRA)*, 2017, pp. 5110–5117.
- [46] E. Malis and E. Marchand, “Experiments with robust estimation techniques in real-time robot vision,” in *2006 IEEE/RSJ Int. Conf. on Intelligent Robots and Systems*, 2006, pp. 223–228.
  - [47] C. Engels, H. Stewénius, and D. Nistér, “Bundle adjustment rules,” *Photogrammetric computer vision*, vol. 2, no. 32, 2006.
  - [48] J. Nocedal and S. Wright, *Numerical optimization*. Springer Science & Business Media, 2006.
  - [49] R. Kümmerle, G. Grisetti, H. Strasdat, K. Konolige, and W. Burgard, “g2o: A general framework for graph optimization,” in *2011 IEEE Int. Conf. on Robotics and Automation*, 2011, pp. 3607–3613.
  - [50] J. Sturm, N. Engelhard, F. Endres, W. Burgard, and D. Cremers, “A benchmark for the evaluation of RGB-D SLAM systems,” in *Proc. of the Int. Conf. on Intelligent Robot Systems (IROS)*, Oct. 2012.
  - [51] R. Mur-Artal, J. M. M. Montiel, and J. D. Tardos, “ORB-SLAM: a versatile and accurate monocular SLAM system,” *IEEE Trans. on robotics*, vol. 31, no. 5, pp. 1147–1163, 2015.